PAPER • OPEN ACCESS

Synthesis and characterization of electro-spun TiO_2 and TiO_2-SnO_2 composite nano-fibers for application in advance generation solar cells

To cite this article: Maham Akhlaq and Zuhair S Khan 2020 *Mater. Res. Express* **7** 015523

Materials Research Express

PAPER

Synthesis and characterization of electro-spun TiO_2 and TiO_2-SnO_2 composite nano-fibers for application in advance generation solar cells

Maham Akhlaq[1] **and Zuhair S Khan**

U.S. Pakistan Center for Advanced Studies in Energy (USPCAS-E), National University of Sciences & Technology (NUST), Islamabad, 44000, Pakistan

[1] Complete postal address: Advanced Energy Materials and Systems Lab., U.S. Pakistan Center for Advanced Studies in Energy (USPCAS-E), National University of Sciences & Technology (NUST), Islamabad, 44000, Pakistan.

E-mail: maham_9458@hotmail.com

Keywords: nano-fibers, electro-spinning, solar cells, titanium oxide, tin oxide

OPEN ACCESS

RECEIVED
31 October 2019

REVISED
23 December 2019

ACCEPTED FOR PUBLICATION
7 January 2020

PUBLISHED
20 January 2020

Abstract

Due to rapid progressive research in the field of nano-technology, nanostructures are attaining tremendous deliberation. Precisely, among these, nano-fibers have accumulated unprecedented attention over the last few years owing to their superior properties such as large surface area to volume ratio. For advance generation solar cells, nano-fibers of metal oxides such as TiO_2 have been widely employed as a working anode but due to the disadvantages of recombination of electrons, their coupling with other metal oxides is necessary to render them useful. This work reports the successful fabrication of TiO_2 , TiO_2/SnO_2 nano-fibers based film and study of the effect of polymer concentration upon it. The crystal structure of synthesized fibers was investigated using XRD, the morphology and chemical composition was analyzed using SEM and EDX, optical properties and chemical properties were studied using UV-VIS spectrophotometer and FT-IR while the electrical properties were studied using Hall Effect measurement system. It was revealed that the prepared TiO_2-SnO_2 nano-fibers exhibit enhanced conductivity, larger band-gap with enhanced photo voltaic properties than TiO_2 nano-fibers. The prepared TiO_2/SnO_2 nano-fibers based solar cells provide an improved efficiency of 4.81% as compared to 1.8% efficiency of bare TiO_2 nano-fibers.

1. Introduction

Material limitations of wafer-based silicon (Si) cell technology and efficiency limitations of thin film solar cell technologies need to be overcome to achieve affordable PV technology [1]. To prevail over these hindrances, advance generation solar cells are a winsome choice. This generation of solar cell encompasses various advantages that can be called upon to expand the range of applications where conventional solar cells are unsuitable. These applications comprises of low light performance, versatile product integration, low energy manufacturing cost [2].

Initially advance generation solar cells utilize bulk semi-conductor materials as their working anode. Bulk semi-conductor materials show photo-corrosion when exposed to sun-light, which decrease the stability of the cells. To reduce this issue, large band-gap nano-structured semi-conductors are employed. These nano-structured semi-conductors exhibit resistance towards photo-corrosion, spectacular optical and electrical properties. Among these nano-structures, nano-fibers have attained marvelous attention in past few years owing to their superior properties. Nano-fibers have found various applications in a variety of fields ranging from medical to high-technology. In advance generation solar cells, metal oxide based nano-fibers are widely used because of their large surface area, high electrical conductivity, fast and unhindered electron transport from photon absorber to FTO, better sensitizer loading and hence improved light-harvesting properties [3].

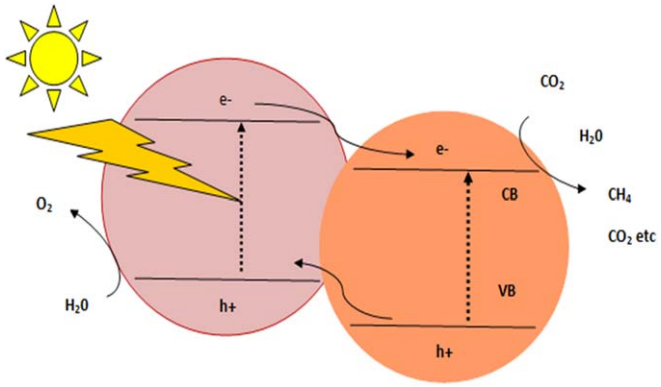

Figure 1. Schematic illustration of a semiconductor hetero-structure.

Metal oxides including TiO_2 [4], SnO_2 [5], ZnO [6] and Nb_2O_3 [7] has been widely grown into such one dimensional nano-structures. Among these oxides, TiO_2 has been extensively employed as electron transport material in most of the advanced generation solar cells mainly Dye-sensitized solar cells[8, 9] , Perovskite solar cells [10] and other hybrid and oxide solar cells [11]. According to Kim et al [12], nano-fibers of TiO_2 possess significant superiority over other nano-structures in term of providing longer one dimensional path for charge transfer, but the increased possibility of recombination of charge carrier's results in the decline in efficiency. Coupling of TiO_2 nano-fibers with other suitable materials can improve its photo-catalytic activities[13] because of the enhancement of charge separation. Various semi-conductor to semi-conductor based hetero-structures of TiO_2 are currently being used including TiO_2/SnO_2 [14], ZnO/SnO_2 [15] and TiO_2/ZnO [16]. Among these hetero-structures, TiO_2/SnO_2 manifests several advantages over others because of the low cost of SnO_2 and some precise crystallographic planes of nano-crystals of TiO_2 and SnO_2. The presence of Sn in the synthesis invariably lowers the average crystallite size. This effect is mainly due to the prevailing surface location of the metal species, which can inhibit the crystal growth [17]. When UV light falls on such structures with photon of energy higher than or equal to the band gaps of TiO_2 and SnO_2, the photo-generated electrons in the irradiated TiO_2 can move to the conduction band (CB) of SnO_2 and the photo-generated holes in the irradiated SnO_2 move to the valence band (VB) of TiO_2 as shown in figure 1. As a result, TiO_2/SnO_2 hetero-structures could hinder the charge recombination and improve the device efficiency. Moreover, band-gap can also be adjusted by using hetero-structures [18].

Nano-fibers can be sensitized using various methods including template-assisted synthesis [19], chemical vapor deposition (CVD) [20], self-assembly [21], wet chemical synthesis [22], and electro-spinning. Electro-spinning is the broadly used technique for nano-fibers synthesis which is further divided into various methods including melt-electro-spinning [23], co-axial electro-spinning, magneto-electro-spinning [24] depending upon the solution and required morphology. Among these synthesis techniques, co-axial electro-spinning utilizes two different precursor solutions that come into contact at the tip and are ejected out of the same needle with high voltage which stretches the droplet into a taylor cone resulting in the formation of core-shell nano-fibers [25]. Electro-spinning utilize polymer as binding material for proper stretching of nano-fibers. Concentration of the polymer solution critically affects the nano-fibers structure.

The aim of this study is to Fabricate, characterize TiO_2 nano-fibers and SnO_2/TiO_2 nano-fibers using co-axial electro-spinning and studied its application in dyesynthesized solar cells. Analysis of morphological, structural, optical as well as electrical properties of the prepared fibers was performed to evaluate their electron transport ability. Study of effect of polymer concentration on structure of prepared fibers was also carried out in this work.

2. Experimental

2.1. Materials

Titanium iso-propoxide ($C_{12}H_{28}O_4Ti$), Poly-vinyl pyrrolidone $(C_6H_9NO)_n$ (M.W = 3,000,000 $g.mol^{-1}$), Stannous chloride di-hydrate $SnCl_2.2H_2O$, Absolute Ethanol (C_2H_5OH), glacial acetic acid (CH_3COOH) were used as raw materials in this study.

Table 1. Prepared Solutions which variable polymer concentrations.

Sample	Ethanol: Glacial Acetic Acid	Titanium iso-propoxide	Stannic chloride Di-hydrate	PVP
T1	1:1	0.5 ml	—	1.4 g
T2	1:1	0.5 ml	—	1.6 g
T3	1:1	0.5 ml	—	1.8 g
TS1	1:1	0.5 ml	0.4 g	1.4 g
TS2	1:1	0.5 ml	0.4 g	1.6 g
TS3	1:1	0.5 ml	0.4 g	1.8 g

2.2. Synthesis of bare TiO_2 nano-fibers and TiO_2/SnO_2 nano-fibers

Titanium iso-propoxide was used as a precursor for synthesizing TiO_2 nano-fibers. Stannic chloride di-hydrate was used as SnO_2 nano-fibers precursor. At first, a homogeneous solution of Ethanol and Glacial acetic acid was made in a ratio of 4:1, by magnetically stirring for 10 min. Various PVP concentrations were added as shown in table 1 to the solution to get a viscous polymeric solution. After stirring the polymer solution for 1 h, 0.5 g of titanium iso-propoxide was added to the solution resulting in a colour transformation to light yellowish hue. The solution was stirred until a homogenous mixture was formed. Following the same methodology such as in case of synthesis of TiO_2 nano-fibers, SnO_2 nano-fibers solution was synthesized by adding 0.2 g of Stannic chloride di-hydrate instead of Titanium iso-propoxide. The solution was stirred until a homogenous mixture was obtained. Different solutions with variable polymer concentration were prepared, as reported in table below.

2.2.1. Electro-spinning setup

The conductive glass (FTO) of dimension of 2 cm^2 x 2 cm^2 was first cleaned thoroughly by sonication in distilled water followed by sonication in ethanol and acetone for 10 min. Cleaned FTO is attached on the top of Aluminium foil which is placed in front of the needle on the collector plate via a conductive carbon tape.

2.2.2. Electro-spinning of solutions

For core-shell nano-fibers, 2 solutions are made which are then subjected to different syringes for nano-fiber synthesis. The highly viscous polymeric solution of TiO_2 and SnO_2 were inserted into 5 ml syringes in a horizontally attached electro-spinning setup. A high voltage of 17.8 kV was attached to this assembly and the solution was injected to the needle at the feed rate of 750 $\mu l\ h^{-1}$. The needle collector distance was set and fixed at 15 cm. A stable taylor cone was acquired which was clearly visible at the tip of the needle. The sample was deposited for 45 min at ambient temperature. The as-spun fibers deposited on FTO and aluminium foil were dried for 1 h at 100 ^oC in a vacuum oven. The heating rate was set at 1^oC/min. The dried nano-fibers were then calcined at 500 ^oC for 1 h in a tube furnace in air. To attain the calcination temperature a heating rate of 3$^\circ C$/min was maintained inside the placement chamber. For both Bare TiO_2 nano-fibers and TiO_2/SnO_2 core shell nano-fibers, 17.8 kV of voltage was applied. The schematic figure of the fabrication of TiO_2/SnO_2 core shell nano-fibers is shown in figure 2. For device fabricated, the prepared nano-fibers of TiO_2 annd TiO_2-SnO_2 composite nano-fibers were coated on indium tin Oxide (ITO) glass having a thin spin coated layer of TiO_2 nano-particles. This thin layer provides better electron transport. The prepared anode was furthermore dipped into N3 dye solution for 20 h for better dye absorption. An ITO glass with a thin layer of gold is used as a counter electrode. The photo-anode with dye is clipped with the gold counter electrode. In the space between the electrodes, a redox electrolyte (I-/I-3) solution was inserted using capillary action. Three set of cells were fabricated for TiO_2 and TiO_2-SnO_2 composite nano-fibers to check repeatability.

2.2.3. Characterization

The electrical conductivity, optical properties, structure and morphology of TiO_2 nano-fibers were characterized by different techniques. The morphology was imaged by using scanning electron microscope (SEM) (Model: Vega3, Tuscan) and elemental composition of the samples was analysed using energy dispersive x-ray spectroscopy. The crystallinity of nano-fibers under consideration was studied using x-ray diffractrometer (Model:Advanced D8,Bruker). The electrical conductivity of the prepared film was measured using Hall Effect measurement system (Ecopia, HMS-3000) while UV-3600 plus UV-VIS NIR Spectrophotometer was used to study its optical properties. For IV measurements, potentiostat system (Biological VSP) was used with a working distance of 8 cm for light intensity similar to sun light.

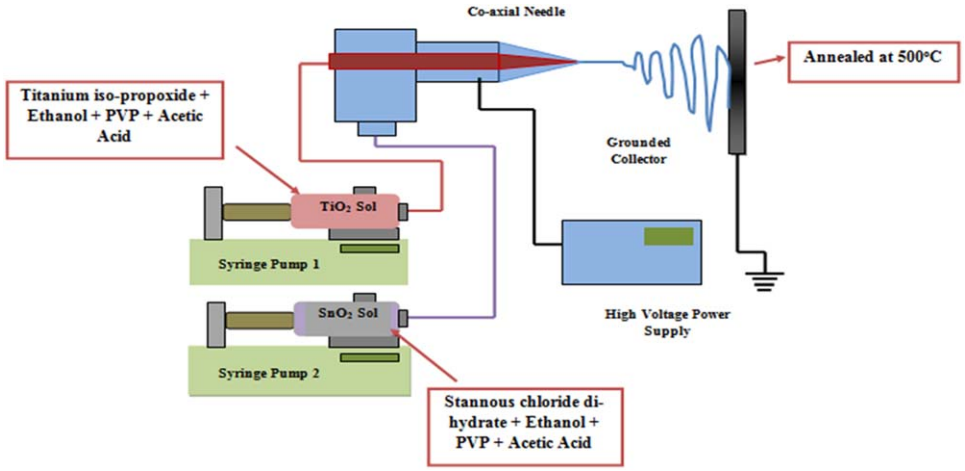

Figure 2. Schematic diagram of fabrication of TiO_2/SnO_2 core shell nano-fibers.

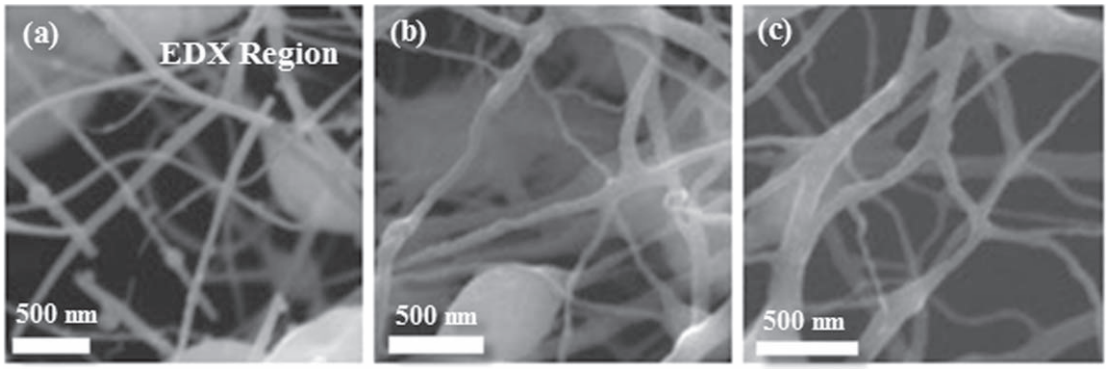

Figure 3. SEM Micrographs of TiO_2 nano-fibers with PVP concentration of (a) 1.4 g (b) 1.6 g (c) 1.8 g.

3. Results and discussions

3.1. Morphological and Elemental Analysis

The high resolution SEM micrographs of TiO_2 and TiO_2/SnO_2 nano-fibers at various polymer concentrations are shown in figures 2 and 3. The average diameter of the finally prepared TiO_2 and TiO_2/SnO_2 nano-fibers is less than the electro-spun nano-fibers before annealing. This effect is perceptible due to the evaporation of solvent and PVP after annealing. During the calcination process, all the organic contents in electro-spun fibers decomposes [26] resulting in morphological change from fibrous to hollow structure [27]. The diameter of TiO_2 nano-fibers and core-shell TiO_2/SnO_2 nano-fibers with 1.4 g, 1.6 g and 1.8 g ranges from 38-48 nm, 50-63 nm, 60-85 nm and 60-120 nm, 70-145 nm and 80-171 nm respectively as shown in figure 5.

As seen in figures 2(a) and 3(a) fibers diameter is smaller however there are various bead structures which are produced due to the high surface tension of the polymer solution. With increase in polymer concentration the Electro-spun solution cause rise in the viscosity of the solution which could persuade the formation of fibers with wider diameter [28]. At high viscosity of the solution, formation of jet is hard which results in the formation of inadequate stretching of the electro-spun solution. This results in the production of wider diameter fibers. Less diameter exhibiting fibers are assumed to offer large surface area to volume ratio, which is expected to reveal better dye absorption in solar cells [29]. Since the dye monolayer is adsorbed on the semiconductor oxide; it is noticeable that its high surface area will enhance the light absorption. The high surface area of nano-fibres provides a remarkable capacity for the attachment or release of dye molecules. With the larger size of the nano-structures, there would be an increase in the light scattering [30].

The round-like/spherical structure confirms the formation of core-shell nano-fibers as shown in figures 4(a)–(c). The un-annealed nano-fibers of TiO_2/SnO_2 nano-fibers in sample with PVP concentration of 1.8 g is shown in figure 5. The fibers are smooth and uniform. There average diameter in this case is larger than the annealed sample. This effect is mainly due to the presence of polymer and other solvent based materials in

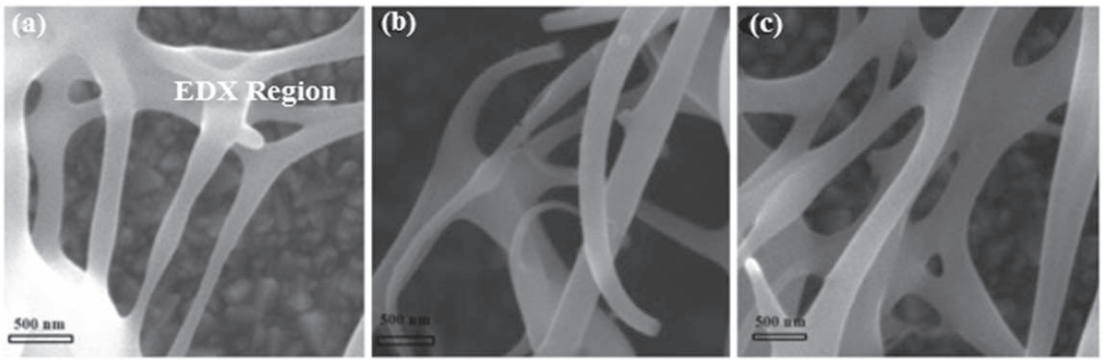

Figure 4. SEM micro-graphs of TiO_2-SnO_2 nano-fibers with PVP concentration of (a) 1.4 g (b) 1.6 g (c) 1.8 g.

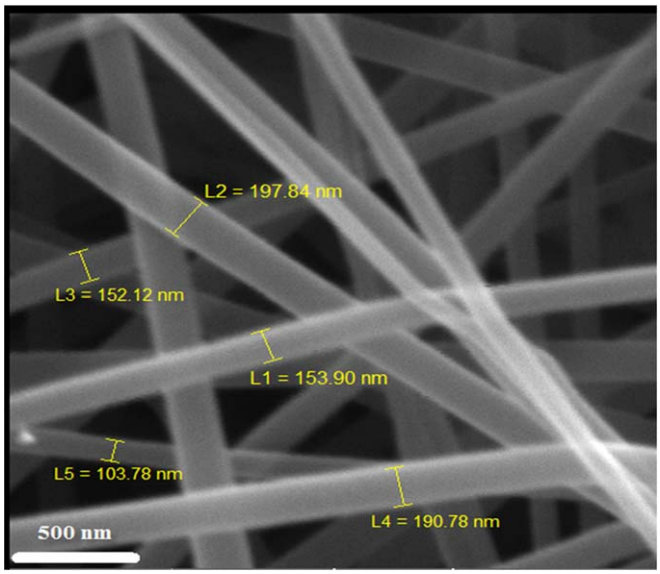

Figure 5. SEM micrographs for TiO_2/SnO_2 nano-fibers with PVP concentration of 1.8 g with-out annealing.

the fibers. After annealing process, only the required metal-oxide based nano-fibers are left. Figure 6(a), (b) shows a plot between the diameter of the fibers with change in polymer concentration.

The presence of Sn in TiO_2/SnO_2 nano-fibers can also be seen in EDS and FT-IR results. The EDS pattern shows prominent peaks of Ti, Sn and O in-case of TiO_2/SnO_2 nano-fibers as shown in figure 7 without traces of any impurities. No traces of carbon in the spectrum show that the PVP is removed completely after annealing process. Presence of high percentage of Sn as shown in table 2, depicts that SnO_2 is successfully encapsulated in TiO2 nano-fibers and of core-shell structure of SnO_2 and $TiO_2$are created [31].

The predictable formation of nano-fibers depends on the experimental mechanism. Among the solvents, glacial acetic acid is used as a catalyst and PVP polymer is used as a binder materials. Polymer materials are however used to give the required molecular weight and concentration for proper stretching of the solution to be electro-spun. Following reaction occurs during the formation of TiO_2 nano-fibers.

$$Ti(OR)_4 + 4R'OH \rightarrow Ti(OH)_4 + 4ROR'$$
$$Ti(OH)_4 + Ti(OH)_4 \rightarrow TiO_2 + H_2O$$

Following reaction occurs during the formation of SnO_2 nano-fibers.

$$SnCl_2.2H_2O + ROH \rightarrow Sn(OH)_4 + RCl$$
$$Sn(OH)_4 \rightarrow SnO_2 + H_2O$$

X-ray Diffraction (XRD) of the synthesized nano-fibers was carried out in order to investigate the crystal phase of TiO_2 and TiO_2/SnO_2 nano-fibres. Figure 8(a) shows the XRD pattern of bare TiO_2 nano-fibers after drying at 100 °C. No evident peaks can be seen in the spectrum, which shows the amorphous behaviour of the TiO_2 nano-fibers film. Similarly the polymer (PVP) has not been evaporated properly. However, figure 8(b)

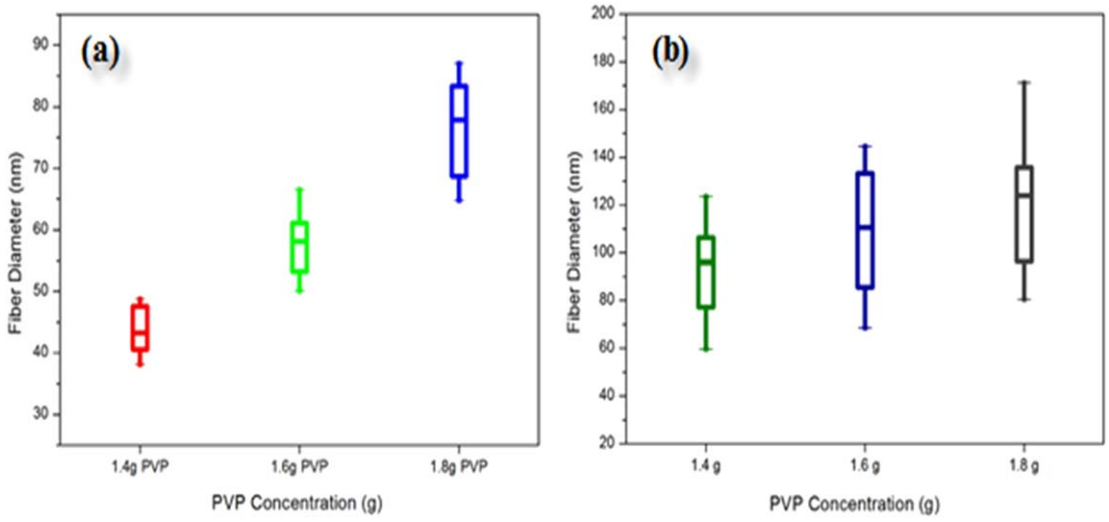

Figure 6. Fiber diameters with various PVP concentrations (a) TiO_2 nano-fibers (b) TiO_2—SnO_2 composite nano-fibers.

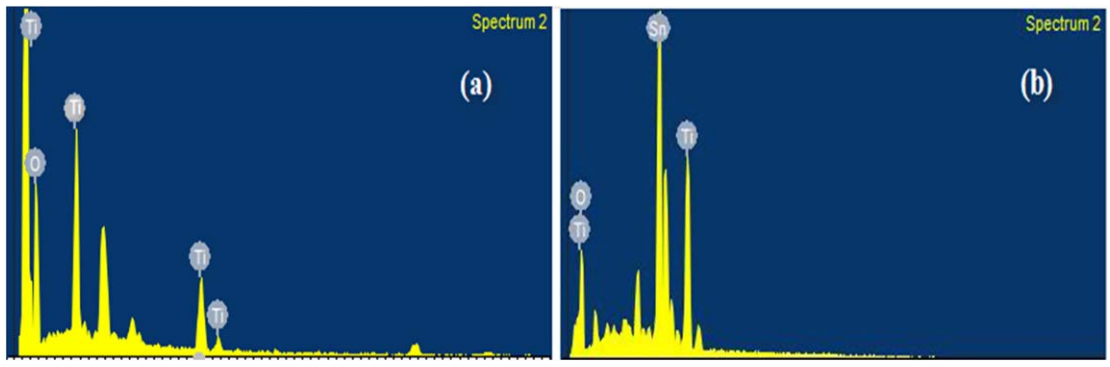

Figure 7. EDX Spectra of annealed (a) TiO_2 nano-fibers (b) TiO_2/SnO_2nano-fibers.

Table 2. Atom % of various elements present in TiO_2 and TiO_2/SnO_2 nano-fibers extracted from EDS Spectrum.

	Atom %		
	Ti	Sn	O
TiO_2 Nano-fibers	12.15	—	87.85
TiO_2/SnO_2 Nano-fibers	9.22	7.86	82.92

demonstrating evident major anatase peaks of TiO_2 as per JCPDS card number 21-1272. The peak at $2\theta = 25.8°$ confirms the formation of TiO_2 anatase structure [32]. The XRD pattern of bare TiO_2 nano-fibers depicts distinctive peaks at $2\Theta = 25.8°, 37.7°, 48.01°, 53.8°$, $55.03°$ and $62.10°$ which can be assigned to (101), (112), (200), (105) , (211) & (204) planes respectively with tetragonal anatase structure. Anatase phase of TiO_2 inherently demonstrate properties like large mobility and wider optical absorption gap. Figure 8(c) shows the addition of 40% SnO_2 in anatase phase of TiO_2, The prominent peaks of (110) , (101) , (211) and other small peaks in figure 7(c) match with the corresponding peaks of tetragonal rutile phase of SnO_2 (JCPDS 41-1445). No additional impurity phase was found, validating the existence of material as a pure nano-composite [33].

Figure 9(a) demonstrated the FTIR spectra of TiO_2/SnO_2 nano-fibers before and after calcination. There are several sharp peaks before annealing. These peaks can be attributed to the presence of polymer and solvent present before annealing. A prominent peak is seen at 1655 cm^{-1} which represent the functional unit of C=O in PVP [33]. The other peak at 1277 cm^{-1} represent C-N bond stretching mode [34]. Moreover peak at around 1400 cm^{-1} represent vibration of CH_2 bond of PVP. A small peak at around 1050 cm^{-1} represents the vibration

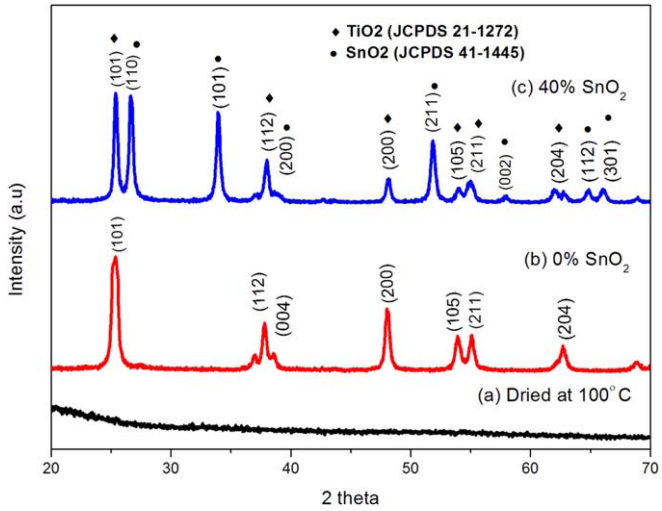

Figure 8. XRD pattern of TiO_2 nano-fibers (a) after drying at 100 °C (b) 0% SnO_2 annealed at 500 °C (c) 40% SnO_2 annealed at 500 °C.

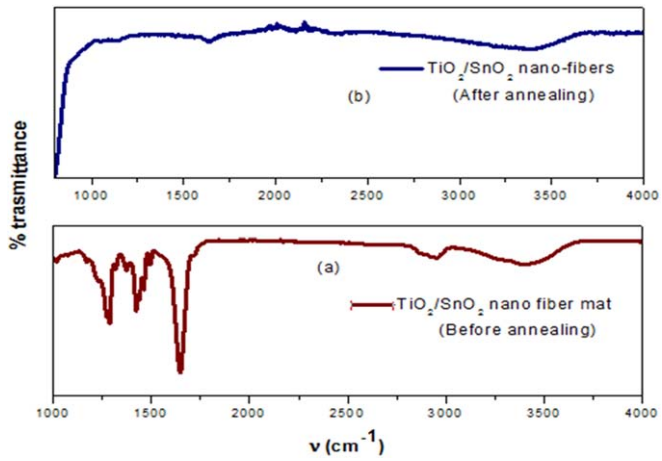

Figure 9. (a) FTIR Spectra of TiO_2-SnO_2 nano-fibers (a) before annealing (b) after annealing.

bend of Ti–O–C. A broad peak in between 3250 cm^{-1} and 3600 cm^{-1} shows the absorption of moisture and solvent during the process of electro-spinning. After annealing there is no major peak in FTIR spectra implying that no impurity exists after the heat treatment [35]. This validate that no water, hydroxyl and hydrocarbon impurity is detected in the IR spectra of calcined TiO_2/SnO_2 nano-fibers [36].

3.2. Optical and electrical properties analysis

The optical properties were studied in wavelength range of 300 nm to 800 nm using UV-VIS NIR spectrophotometer. In the absorption spectrum of TiO_2-SnO_2 nano-fibers, a blue shift was observed as compared to TiO_2 nano-fibers; such a shift can be attributed to the in-corporation of SnO_2 [36].

The band-gap (E_g) of the prepared materials was calculated by using tauc plot; $\alpha h\upsilon = A(h\upsilon\text{-}E_g)^n$ [37]. where A is the absorption coefficient calculated from UV VIS absorption spectra shown in figure 10, h is the plank constant, υ is the frequency which is equals to $\upsilon = 3 \times 10^8/\lambda$, A is a contact and $n = 1/2$ referred to direct allowed transition. Tauc plot is drawn between the photon energy $h\upsilon$ (eV) and direct band-gap $(\alpha h\upsilon)^2$. The calculated band-gap of TiO_2-SnO_2 nano-fibers is 3.81 eV as compared to the band-gap of TiO_2 nano-fibers of 3.52 eV. This increase in band-gap means increase in Fermi level and open circuit voltage for a typical DSSC solar cell. Moreover it facilitates electron transfer from excited state of electron to the external circuit [38].

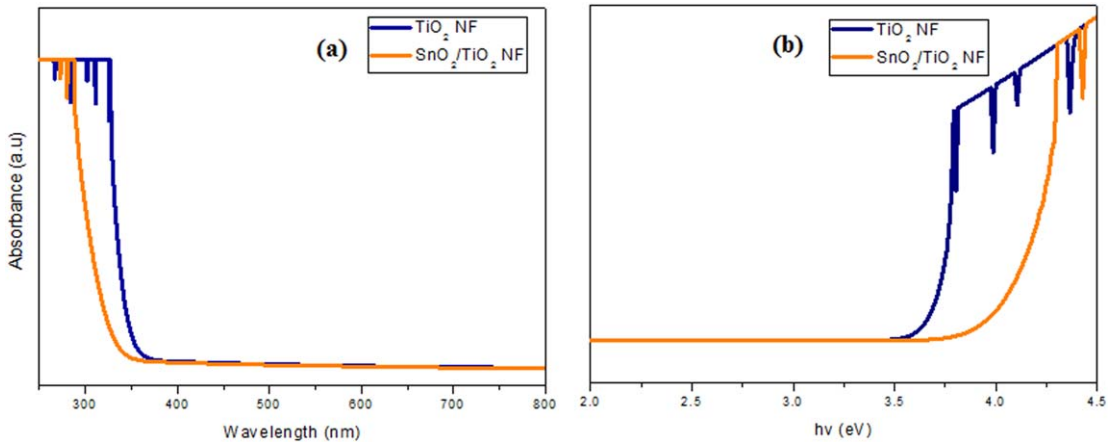

Figure 10. Prepared TiO_2 nano-fibers and TiO_2-SnO_2 nano-fibers (a) UV-Vis absorption spectra (b) Tauc Plot.

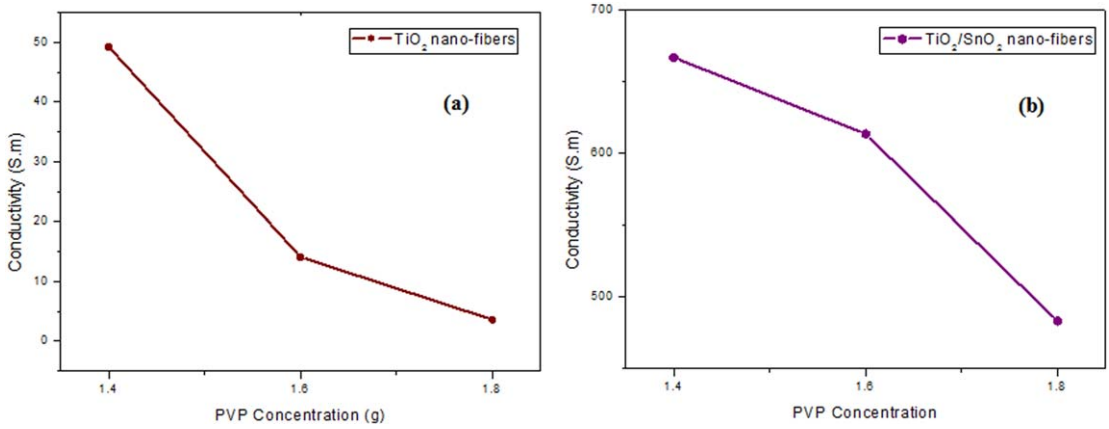

Figure 11. Conductivity of the film prepared with variable PVP concentration (a) TiO_2 nano-fibers (b) TiO_2/SnO_2 nano-fibers.

3.3. Electrical measurements

The Electrical property including conductivity of the annealed nano-fibers deposited on FTO (conductive glass) was studied using Hall Effect measurement system. The conductivity of TiO_2-SnO_2 nano-fibers is found to be higher than that of bare TiO_2 nano-fibers as shown in figure 11. The conductivity of TiO_2 nano-fibers and TiO_2/SnO_2 nano-fibers was calculated to be 1.831E-02 S.m and 1.407E + 01 S.m respectively. This is primarily because of the addition of SnO_2 to TiO_2 nano-fibres. Addition of SnO_2 stabilizes the anatase phase of TiO_2. Similarly with addition of SnO_2 the number density of the fibers increases, as a result of rise of the fibers with variable diameter. The hetro-structure of TiO_2/SnO_2 will also facilitate charge separation which results in the reduction of recombination of electrons. The electrons in TiO_2 will flow to SnO_2, because the work function of TiO_2 is smaller than SnO_2. This phenomenon can result in an increase of the electrons concentration in the SnO_2 layer, which results in an increase in conductivity of the film. Similarly with increase in nano-fiber diameter, the conductivity of the film decrease as shown in figure 10. The decrease is conductivity can be attributed to the geometric surface and packing density effect. The working anode of solar cell should have high conductivity to facilitate the movement of electron from photon absorber to the external circuit easily [39].

3.4. Photovoltaic performance of DSSC

The effect of nano-fibers diameter on photovoltaic performance of DSSC was studied. The fill factor and the efficiency of the prepared cell were calculated using the V_{oc} and J_{sc}. As shown in figure 12, thinner diameter nano-fibers based DSSC shows better performance due to larger surface area to volume ratio. The results in better dye absorption and more efficiency of electron transfer. The large beads form in high viscous solution results in light scattering which produce less efficient solar cells. Moreover, with the incorporation of SnO_2 in TiO_2 nano-fibers, efficiency increases. This effect is due to the better charge separation for electron transport throughout the circuit.

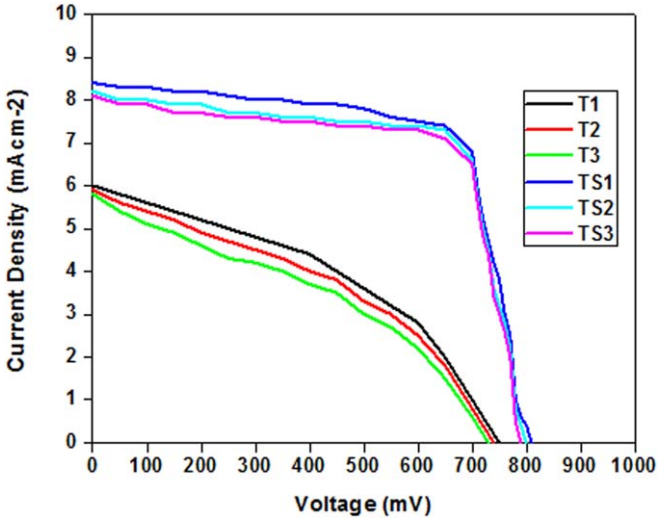

Figure 12. Comparison of IV Measurements of TiO_2 and TiO_2/SnO_2 with various polymer concentrations.

Table 3. Comparison of photo-voltaic parameters (Voc , Isc, FF and η) for TiO_2 and TiO_2/SnO_2 nano-fibers samples with different PVP concentration.

Sample	V_{oc} (V)	J_{sc}(mAcm^{-2})	Fill factor	Efficiency η(%)
T1	0.75	6	0.4	1.8
T2	0.74	5.9	0.38	1.63
T3	0.72	5.9	0.29	1.33
TS1	0.81	8.4	0.70	4.81
TS2	0.8	8.2	0.70	4.6
TS3	0.78	8	0.69	4.46

Table 4. Benchmark table between Literature and this work.

Reference	Material	^{J}sc (mAcm^{-2})	V_{oc} (V)	Efficiency η(%)
P F Du (2014) [40]	TiO_2 Nano-particles/Nano-fibers	10.6	0.70	4.46
Wali (2016) [41]	SnO_2 nano-fibers/TiO_2 nano-fibers	18.0	0.57	4.5
Lim (2016) [42]	Hierarchical TiO_2–SnO_2 Nano-composite	12.68	0.61	3.73
Zhang (2016) [43]	Mesoporous TiO_2 nano-fibers	3.937	0.915	1.82
Altaf (2019) [44]	TiO_2 nano-fiber	8.99	0.738	4.09
This work	TiO_2/SnO_2 composite core shell nano-fibers	8.4	0.81	4.81

By calculating Fill factor the efficiency of the in house prepared solar cells was studied. The table 3 shows that a change in the fiber diameter results in a change in efficiency of the cell. For sample T1 with 1.2 g PVP concentration, the overall efficiency of the cell is 1.8%. However with increase in polymer concentration to 1.8 g, the efficiency decreases to 1.33%. This effect is because of the beads produced due to high polymer concentration. However by the addition of SnO_2 to TiO_2 nano-fibers, the overall solar cell efficiency can be enhanced to 4.81%. However, the effect of polymer concentration is also valid in TiO_2/SnO_2 nano-fibers. The increase in the value of J_{sc} depicts a better diffusion and injection of electrons which provide better dye absorption and electron transfer in advance generation solar cells.

Table 4 shows a comparison between this work and the latest literature. The core shell nano-fibers based DSSC in comparison with other literature shows an enhanced power conversion efficiency of 4.81%. The efficiency can furthermore be enhanced by studying the effect of change of SnO_2 precursor concentration in TiO_2/SnO_2 core shell nano-fibers based DSSC. Moreover the effect of change of diameter mainly due to other process parameters including voltage, flow rate, collector to needle distance can also be studied.

4. Conclusion

In this work, TiO_2 and TiO_2-SnO_2 nano-fibers were successfully synthesized using solution electro-spinning and co-axial electro-spinning methods, to be employed as active anode for advance generation solar cells. The diameter of the fibers is found to be less than 200 nm. XRD Pattern confirms the formation of anatase TiO_2 and tetragonal rutile phase of SnO_2. Furthermore, the morphological analysis reveals the hollow structure of nano-fibers. Study of effect of polymer concentration upon nano-fibers synthesis demonstrated that increase in polymer concentration results in the increase in diameter by approximately a quarter. FTIR results validated that no water, hydroxyl group or hydrocarbons are present after annealing. Moreover, UV-VIS spectral data signifies that there has been a significant increase in band-gap in case of TiO_2-SnO_2 nano-fibers in comparison with bare TiO_2 nano-fibers. The electrical properties of the prepared films calculated using Hall Effect measurement also showed promising results denoting high conductivity values of TiO_2-SnO_2 nano-fibers film with an efficiency of 4.81% which making them undoubtedly suitable for future solar cell technologies and applications.

Acknowledgments

Authors wish to thank US Pakistan Centre for advance studies in Energy and PGP NUST for their financial support to carry out this research. Special thanks to people at AEM&S Lab at USPCAS-E for the assistance to carry out the research work.

ORCID iDs

Maham Akhlaq https://orcid.org/0000-0002-9883-8631

References

[1] Solanki C S and Beaucarne G 2007 Advanced solar cell concepts *Energy Sustain. Dev.* **11** 17–23
[2] Nazeeruddin M K, Baranoff E and Grätzel M 2011 Dye-sensitized solar cells: a brief overview *Sol. Energy* **85** 1172–8
[3] Muduli S *et al* 2009 Enhanced conversion efficiency in dye-sensitized solar cells based on hydrothermally synthesized TiO_2-MWCNT nanocomposites *ACS Appl. Mater. Interfaces* **1** 2030–5
[4] Suryana R, Rahmawati L R and Triyana K 2016 Growth of TiO_2 nanofibers on FTO substrates and their application in dye-sensitized solar cells *J. Phys. Conf. Ser.* **776** 012006
[5] Zhang S, Yin B, Jiao Y, Liu Y, Qu F and Wu X 2014 Nanosheet based SnO_2 assembles grown on a flexible substrate *Appl. Surf. Sci.* **305** 626–9
[6] Martinson A B F, Elam J W, Hupp J T and Pellin M J 2007 ZnO nanotube based dye-sensitized solar cells *Nano* **7** 2183–7
[7] Ghosh R *et al* 2011 Nanoforest Nb_2O_5 photoanodes for dye-sensitized solar cells by pulsed laser deposition *ACS Appl. Mater. Interfaces* **3** 3929–35
[8] Han Z, Zhang J, Yu Y and Cao W 2012 A new anode material of silver photo-deposition on TiO_2 in DSSC (c) *Mater. Lett.* **70** 193–6
[9] Ko K H, Lee Y C and Jung Y J 2005 *Enhanced efficiency of dye-sensitized TiO_2 solar cells (DSSC) by doping of metal ions* **283** 482–7
[10] Ke W, Fang G, Wang J, Qin P, Tao H, Lei H, Liu Q, Dai X and Zhao X 2014 Perovskite Solar Cell with an Efficient TiO_2 Compact Film *ACS Appl. Mater. Interfaces* **6** 15959–65
[11] Pei J, Hao Y Z, Lv H J, Sun B, Li Y P and Guo Z M 2015 Optimizing the performance of TiO_2/P3HT hybrid solar cell by effective interfacial modification *Chem. Phys. Lett.* **644** 127–31
[12] Kim H H, Park C, Choi W, Cho S, Moon B and Son D I 2014 *Dye-sensitized Solar Cells* **65** 1315–9
[13] Sadeghi M, Liu W, Zhang T-G, Stavropoulos P and Levy B 1996 Role of photoinduced charge carrier separation distance in heterogeneous photocatalysis: oxidative degradation of CH_3OH vapor in contact with Pt/TiO_2 and cofumed TiO_2 −Fe_2O_3 *J. Phys. Chem.* **100** 19466–74
[14] Cao Y *et al* 2000 A bicomponent TiO_2/SnO_2 particulate film for photocatalysis *Chem. Mater.* **12** 3445–8
[15] Liu Z-Q *et al* 2012 ZnO/SnO_2 hierarchical and flower-like nanostructures: facile synthesis, formation mechanism, and optical and magnetic properties *CrystEngComm* **14** 2289
[16] Yang M *et al* 2017 TiO_2 nanoparticle/nanofiber–ZnO photoanode for the enhancement of the efficiency of dye-sensitized solar cells *RSC Adv.* **7** 41738–44
[17] Deepak T G, Anjusree G S, Thomas S, Arun T A, Nair S V and Nair A S 2014 A review on materials for light scattering in dye-sensitized solar cells *RSC Adv.* **4** 17615–38
[18] Dürr M, Rosselli S, Yasuda A and Nelles G 2006 Band-gap engineering of metal oxides for dye-sensitized solar cells *J. Phys. Chem.* B **110** 21899–902
[19] Liu Y, Goebl J and Yin Y 2013 Templated synthesis of nanostructured materials *Chem. Soc. Rev.* **42** 2610–53
[20] Chi M, Zhao Y, Fan Q and Han W 2014 The synthesis of PrB6 nanowires and nanotubes by the self-catalyzed method *Ceram. Int.* **40** 8921–4
[21] Kovtyukhova N I, Martin B R, Mbindyo J K N, Mallouk T E, Cabassi M and Mayer T S 2002 Layer-by-layer self-assembly strategy for template synthesis of nanoscale devices *Mater. Sci. Eng.* C **19** 255–62
[22] Zhu H, Gao X, Lan Y, Song D, Xi Y and Zhao J 2004 Hydrogen titanate nanofibers covered with anatase nanocrystals: a delicate structure achieved by the wet chemistry reaction of the titanate nanofibers *J. Am. Chem. Soc.* **126** 8380–1
[23] Larrondo L and Manley R S J 1981 Electrostatic fiber spinning from polymer melts. II. Examination of the flow field in an electrically driven jet *Polym. Sci. Polym.* **19** 921–32

[24] He J-H, Liu Y, Mo L-F, Wan Y-Q and Xu L 2008 Electrospun nanofibres and their applications *iSmithers, Shawbury, Shrewsbury, Shropshire, UK* p 260
[25] Wu Y, Yu J Y, He J H and Wan Y Q 2007 Controlling stability of the electrospun fiber by magnetic field *Chaos Solitons Fractals* **32** 5–7
[26] Nuansing W, Ninmuang S, Jarernboon W, Maensiri S and Seraphin S 2006 Structural characterization and morphology of electrospun TiO_2 nanofibers *Mater. Sci. Eng. B Solid-State Mater. Adv. Technol.* **131** 147–55
[27] a Kumar R, Jose K, Fujihara J, Wang and Ramakrishna S 2007 Structural and optical properties of electrospun TiO_2 nanofibers *Chem. Mater.* **19** 6536–42
[28] Sheng T Z, Nurmin B, Ismail S and Lynn A J 2016 The morphology of electrospun titanium dioxide nanofibers and its influencing factors *MATEC Web of Conferences* **46** 1–7
[29] Chem J M 2012 Effect of TiO_2 morphology on photovoltaic performance of dye-sensitized solar cells : nanoparticles , nanofibers, hierarchical spheres and ellipsoid *J. Mater. Chem.* **22** 7910–8
[30] Jeng M-J, Wung Y-L, Chang L-B and Chow L 2013 Particle size effects of TiO_2 layers on the solar efficiency of dye-sensitized solar cells *Int. J. Photoenergy* **2013** 1–9
[31] Ba-Abbad M M, Kadhum A A H, Mohamad A B, Takriff M S and Sopian K 2012 Synthesis and catalytic activity of TiO_2 nanoparticles for photochemical oxidation of concentrated chlorophenols under direct solar radiation *Int. J. Electrochem. Sci.* **7** 4871–88
[32] Li F, Gao X, Wang R, Zhang T, Lu G and Barsan N 2016 Design of core-shell heterostructure nanofibers with different work function and their sensing properties to trimethylamine *ACS Appl. Mater. Interfaces* **8** 19799–806
[33] Soltani N *et al* 2012 Influence of the polyvinyl pyrrolidone concentration on particle size and dispersion of ZnS nanoparticles synthesized by microwave irradiation *Int. J. Mol. Sci.* **13** 12412–27
[34] Wang M, Song Y, Wang M, Zhang X, Wu J and Zhang T 2014 Investigation on the role of the molecular weight of polyvinyl pyrrolidone in the shape control of high-yield silver nanospheres and nano-wires *Nanoscale Res. Lett.* **13** 1–8
[35] Mohamed I M A, Dao V D, Yasin A S, Choi H S and Barakat N A M 2016 Synthesis of novel SnO_2@TiO_2nanofibers as an efficient photoanode of dye-sensitized solar cells *Int. J. Hydrogen Energy* **41** 10578–89
[36] Mohamed I M A, Dao V D, Yasin A S, Choi H S, Khalil K A and Barakat N A M 2017 Facile synthesis of GO@SnO_2/TiO_2 nanofibers and their behavior in photovoltaics *J. Colloid Interface Sci.* **490** 303–13
[37] Yoo D, Kim I, Kim S, Hie C, Lee C and Cho S 2007 Effects of annealing temperature and method on structural and optical properties of TiO_2 films prepared by RF magnetron sputtering at room temperature *Appl. Surf. Sci.* **253** 3888–92
[38] Hagfeldt A, Boschloo G, Sun L, Kloo L and Pettersson H 2010 Dye-sensitized solar cells *Chem. Rev.* **110** 6595–663
[39] Gong J, Liang J and Sumathy K 2012 Review on dye-sensitized solar cells (DSSCs): fundamental concepts and novel materials *Renew. Sustain. Energy Rev.* **16** 5848–60
[40] Du P, Song L X and Xiong J 2014 Enhanced conversion efficiency in Dye-sensitized solar cells based on bilayered nano-composite photoanode film consisting of TiO_2 nanoparticles and nanofibers *J. Nanosci. Nanotechnol.* **14** 4164–9
[41] Wali Q, Fakharuddin A, Ahmed I, Ab Rahim M H, Ismail J and Jose R 2014 Multiporous nanofibers of SnO_2 by electrospinning for high efficiency dye-sensitized solar cells *J. Mater. Chem.* A **2** 17427–34
[42] Lim C K, Wang Y and Zhang L 2016 Facile formation of a hierarchical TiO_2-SnO_2 nanocomposite architecture for efficient dye-sensitized solar cells *RSC Adv.* **6** 25114–22
[43] Zhang W, Zhu R, Ke L, Liu X, Liu B and Ramakrishna S 2010 Anatase mesoporous TiO_2 nanofibers with high surface area for solid-state dye-sensitized solar cells *Small* **6** 2176–82
[44] Altaf A A, Ahmed M, Hamayun M, Kausar S, Waqar M and Badshah A 2019 Titania nano-fibers : a review on synthesis and utilities *Inorganica Chim. Acta* **501** 119268